von Willebrand disease-specific defects and proteomic signatures in endothelial colony-forming cells

Laan, S.N.J.; Groten, S.; Dirven, R.J.; Bürgisser, P.E.; Leebeek, F.W.G.; Moort, I. van; ... ; SYMPHONY consortium

Received: 2 December 2024 | Revised: 30 March 2025 | Accepted: 23 April 2025

https://doi.org/10.1016/j.jtha.2025.04.024

ORIGINAL ARTICLE

von Willebrand disease-specific defects and proteomic signatures in endothelial colony–forming cells

Sebastiaan N. J. Laan[1,2] | Stijn Groten[3] | Richard J. Dirven[1] | Petra E. Bürgisser[2] | Frank W. G. Leebeek[2] | Iris van Moort[2] | Maartje van den Biggelaar[3] | Ruben Bierings[2] | Jeroen Eikenboom[1] | for the SYMPHONY consortium

[1]Department of Internal Medicine, Division of Thrombosis and Hemostasis, Leiden University Medical Centre, Leiden, the Netherlands

[2]Department of Hematology, Erasmus University Medical Centre, Rotterdam, the Netherlands

[3]Department of Molecular Hematology, Sanquin Research, Amsterdam, the Netherlands

Correspondence
Jeroen Eikenboom and Sebastiaan N. J. Laan, Department of Internal Medicine, Division of Thrombosis and Hemostasis, Leiden University Medical Center, P.O. Box 9600, 2300 RC Leiden, the Netherlands.
Email: h.c.j.eikenboom@lumc.nl and s.n.j.laan@lumc.nl

Funding information
Funding by SYMPHONY: NWO-NWA.1160.18.038 (received by S.N.J.L., I.v.M., R.B., and J.E.), and Landsteiner Foundation for Blood Transfusion Research, Grant Number: 1707 (received by R.B.).

Abstract

Background: Endothelial cells are crucial for hemostasis as they produce von Willebrand factor (VWF). von Willebrand disease (VWD) results from a deficiency of, or defects in, VWF.

Objectives: We analyzed the endothelial compartment of VWD patients with an unexplained decrease in VWF level or nonresponse to 1-8-deamino-D-arginine vasopressin (DDAVP) using endothelial colony–forming cells (ECFCs).

Methods: Thirteen healthy controls and 10 VWD type 1 and 2 patients were included, and a total of 29 ECFC clones were obtained. Plasma was analyzed, and ECFCs were morphologically and functionally characterized by quantitative polymerase chain reaction, ELISA, imaging, migration assay, and mass spectrometry.

Results: VWF plasma levels were reduced in all patients. ECFCs were categorized into 2 previously defined transcriptional clusters and matched between patients and controls. Four ECFC clones, all from DDAVP nonresponders, retained VWF in the endoplasmic reticulum. Cluster 1 ECFCs from DDAVP nonresponders closed more slowly in the migration assay and had lower basal release of VWF antigen than control ECFCs. Proteomic data of ECFC lysates showed overlap in clustering with RNA profiles, including ALDHA1, TGFB1, and other endothelial-to-mesenchymal/inflammatory markers. However, no patient group-specific phenotype was observed. Finally, regulated secretion of VWF and Weibel–Palade body count in ECFCs correlated with various secretory machinery components.

Conclusion: Lower plasma VWF was linked to reduced production and secretion by ECFCs obtained from patients. Furthermore, nonresponse to DDAVP in some patients was explained by VWF retention in the endoplasmic reticulum. The correlation

Manuscript handled by: Karen Vanhoorelbeke

Final decision: Karen Vanhoorelbeke, 23 April 2025

Sebastiaan N. J. Laan and Stijn Groten share first authorship.

Ruben Bierings and Jeroen Eikenboom share last authorship.

between functional aspects of ECFCs and their quantitative polymerase chain reaction and proteome profiles yielded potential targets for further research.

KEYWORDS
endothelial cells, hemostasis, mass spectrometry, von Willebrand diseases, von Willebrand factor

1 | INTRODUCTION

Endothelial cells play a key role in hemostasis. von Willebrand factor (VWF) is one of the main components of primary hemostasis and is produced by endothelial cells and megakaryocytes. VWF is a large multimeric glycoprotein that binds to collagen and platelets, thereby initiating platelet plug formation upon vessel damage. VWF also binds to factor (F)VIII and protects it from degradation. The protein is stored in specialized cigar-shaped secretory organelles called Weibel–Palade bodies (WPBs) [1,2]. These organelles can secrete their content continuously into the vessel, which provides a steady level of VWF. However, endothelial cells can also be stimulated by injury or stress to rapidly secrete their content to increase VWF levels locally [3].

When VWF is deficient or qualitatively defective, bleeding can occur, known as von Willebrand disease (VWD) [4]. This is the most common inherited bleeding disorder in humans, found in approximately 1 in 100 individuals [5]. The disease can be divided into 3 subtypes. Type 1 is hallmarked by low levels of functionally normal VWF, whereas in type 3, VWF is not present at all, making it the most severe type. Type 2 VWD is associated with qualitative defects in VWF, like impaired multimerization (type 2A), enhanced or spontaneous binding to platelets (type 2B), decreased binding to platelets or collagen (type 2M), or decreased binding to FVIII (type 2N) [4]. VWD is usually treated by either administration of 1-8-deamino-D-arginine vasopressin (DDAVP) or VWF concentrates [6]. However, large interindividual differences in response to DDAVP are observed. Several studies have reported differences in response due to disease subtype, variant, age, or blood group [7–20], but the cause of the variation is not fully understood. Although VWD is the most common bleeding disorder, it is difficult to diagnose due to the large heterogeneity and number of variants or deletions in the *VWF* gene observed within patients [21]. Adding to the complexity, roughly 30% to 50% of VWD type 1 patients do not have *VWF* gene variants and have been shown to present with a distinctly different bleeding phenotype [22–24]. Current assays and genetic testing often do not explain the cause of bleeding in these patients, and it is hypothesized that other modifiers cause the low levels and associated bleeding [25].

As endothelial cells are vital in the synthesis, storage, and secretion of VWF, we hypothesized that they may play a role in the unexplained VWD phenotype of patients without *VWF* variant and may yield insight into the cause of the poor response to DDAVP. One way to study the molecular and pathophysiological aspects of patient endothelial cells is the endothelial colony–forming cell (ECFC) model. One significant benefit of this model is its capability to generate clonally proliferative cells that exhibit endothelial traits, including the production and storage of VWF within WPBs, response to stimuli, and characteristic endothelial cobblestone-like morphology [26]. When obtained from patients, these cells can be used to study the pathophysiological mechanisms of VWD in patients [27–31].

In this study, we aimed to investigate the endothelial compartment in the context of VWD, as the endothelial cells may play a role in the unexplained low levels of VWF or poor DDAVP response in some patients. We found distinct retention of VWF in the endoplasmic reticulum (ER) in the ECFCs of some patients who did not respond to DDAVP. Furthermore, we highlight the inverse correlation between secreted VWF antigen (VWF:Ag) by ECFCs after stimulation and WPB count with cell area, and the correlation between VWF levels and exocytotic machinery.

2 | MATERIALS AND METHODS

2.1 | Patient inclusion and ethical approval

Patients were selected from the previous nationwide cross-sectional Willebrand in the Netherlands (WiN) study [32]. Informed consent was obtained from 10 patients and 13 healthy donors. Healthy donors had not been diagnosed with VWD or any other bleeding disorder. Inclusion criteria for the patients were as follows: diagnosed with VWD and either 1) no identified *VWF* variants, as measured in the WiN study, or 2) with a *VWF* variant but nonresponsive to DDAVP. Complete response was defined as 2 times increase in VWF platelet binding activity (VWF:Act) from baseline at 1 hour after DDAVP and VWF:Act $\geq$ 50 IU/dL until 4 hours after DDAVP [32]. At the moment of inclusion, the International Society on Thrombosis and Haemostasis Bleeding Assessment Tool [33] was obtained, and blood samples were drawn (10 mL citrated and 50 mL heparinized blood).

2.2 | Plasma coagulation factor levels

Citrated plasma samples from patients and controls at the time of inclusion were centrally measured for VWF:Ag, VWF:Act, VWF collagen binding (VWF:CB), and FVIII coagulant activity. The assays that were used for these central measurements are described in the Supplementary Methods. Furthermore, from the WiN database,

historically lowest plasma levels and levels at the time of inclusion in the WiN study were also used in this study [32]. Note that historical VWF activity was measured with different platelet binding assays. In this article, all VWF activity levels are indicated as VWF:Act.

2.3 | ECFC generation

ECFCs were obtained following study protocols, which were approved by the Leiden University Medical Center and Erasmus University Medical Center (EMC) ethics review boards. Isolation and cell culture of ECFCs were performed as described previously [34] based on the original protocol [35]. In short, isolation and culture procedures involved venipuncture to collect whole blood, isolation of peripheral blood mononuclear cells, and subsequent culture in endothelial growth medium (EGM)-18; (EBM-2 Basal Medium with EGM-2 supplements and growth factors; Lonza or PromoCell) with 18% heat-inactivated fetal bovine serum (Thermo Fisher Scientific). At the EMC, non–heat-inactivated fetal bovine serum was used. Clones typically emerged between days 10 and 21 and were frozen upon reaching confluency in 3 T75 flasks (at Leiden University Medical Center) or 4 T75 flasks (at EMC) at passage 3. A total of 29 clones were isolated in this study, with experiments conducted on clones at passage 5. Detailed information regarding each clone is provided in Table.

2.4 | Brightfield and immunofluorescence image acquisition

For brightfield imaging, ECFCs at passage 5 were imaged 3 days after confluency was reached with the Leica MC170 HD camera attachment to a DM IL LED (2.5× and 5× lens; Leica). For immunofluorescence imaging, staining and imaging were performed as described before [36]. All samples were stained with antibodies against VWF and VE-cadherin, and nuclei were stained with Hoechst diluted in blocking buffer. In addition, ER was visualized by staining with antibodies against protein disulfide isomerase. See Supplementary Table S1 for details on antibodies. Imaging for large tile scans was performed similarly, as described before [36], although a 5 × 5 tile scan was made for a total area of 1059.84 × 1059.84 μm (23261 μm^2). For superresolution imaging, cells were imaged using the Zeiss LSM900 Airyscan2 upright confocal microscope with a 63× oil immersion objective.

2.5 | Migration assay and image acquisition

For the cell migration assay, all samples were cultured in 48-well plates at passage 5. The protocol was followed as described previously [36]. Briefly, each clone was randomly plated in 6 wells of a 48-well plate. Three days after confluency was reached, cells were labeled with CellTracker Green (Life Technologies) diluted 1:10 000 in EGM-18 medium for 45 minutes. Three wells per clone were treated with 12.5 μg/mL mitomycin C (Sigma–Aldrich) for 2 hours, while the remaining 3 wells received medium only. The confluent cell layer was damaged by making a scratch using a p100 pipette tip, after which the cells were imaged using the AF6000 microscope (Leica) with a 10× lens at 37 °C and 5% CO_2. Each well was imaged every 30 minutes for 24 hours for visualization of cell migration. Time points 1, 2, and 3 had to be removed from analysis due to shifting of the plate during image acquisition.

2.6 | Automated quantification of ECFC morphology and migration

Automated quantification of ECFC parameters was done mostly with CellProfiler (version 4.2.1) [37]. Confocal imaging tile scans of ECFCs were analyzed using the purpose-made OrganelleProfiler pipeline as described previously [38]. The pipeline was optimized as needed for the antibodies used and the measured intensity. For the current study, we adjusted the OrganelleProfiler pipeline so that artifacts with high intensity, usually 6 to 7 times >VWF signal, were identified and masked out of the image prior to WPB analysis. For the migration assay analysis, a previously developed CellProfiler pipeline was used to identify, count, and track individual cells [36]. Analysis parameters and pipeline modifications specific to this study are detailed in the Supplementary Methods. The CellProfiler pipelines used for morphology and migration analysis are supplied in Supplementary Files S1 and S2 and are made available on GitHub (https://github.com/Clotterdam).

2.7 | Basal and stimulated release of VWF

Basal release of VWF in EGM-18 medium by ECFCs was determined by collecting cell culture supernatants over 24 hours as described previously [34]. To determine Ca^{2+}- and cyclic adenosine monophosphate-mediated regulated release of VWF (further referred to as stimulated release), cells were stimulated with 100 μM histamine (Sigma–Aldrich) or 10 μM epinephrine (Sigma–Aldrich) and 100 μM IBMX (Sigma–Aldrich) for 1 hour [34,39], respectively. Cell culture supernatants of the stimulated cells were then collected. Cells were then lysed to collect intracellular VWF. Finally, media and lysates were measured by VWF:Ag enzyme-linked immunosorbent assay as described previously [40].

2.8 | Mass spectrometry sample preparation, acquisition, and analysis

For mass spectrometry analysis of endothelial cell (EC) proteomes, samples were digested with trypsin as described previously [41]. Tryptic digests were transferred to an Evotip Pure (Evosep) according to manufacturer's guidelines and analyzed with an Evosep One liquid chromatography system (Evosep) coupled to a timsTOF HT mass spectrometer (Bruker). Peptides were separated on a 15 cm × 150 μm, 1.5 μm Performance Column (EV1137 from EvoSep) with a

TABLE Patient and control endothelial colony–forming cell characteristics.

ID	Diagnosis	DNA change	Protein change	Age at inclusion	Sex	Blood group	ISTH-BAT bleeding score	Hist. lowest VWF:Ag (U/dL)	Hist. lowest VWF:Act (U/dL)	Sample no.	Day of detection[b]	Time in culture[c]	Cluster
1	Control	n.d.	n.a.	22	Female	O	0	n.d.	n.d.	S2	13	10	1
										S4	13	11	1
2	Control	n.d.	n.a.	28	Female	n.d.	n.d.	n.d.	n.d.	S6	19	30	1
3	Control	n.d.	n.a.	29	Female	O	4	n.d.	n.d.	S12	21	38	2
4	Control	n.d.	n.a.	23	Female	n.d.	n.d.	n.d.	n.d.	S14	13	23	2
										S20	15	27	2
5	Control	n.d.	n.a.	27	Female	O	0	n.d.	n.d.	S18	14	44	2
6	Control	n.d.	n.a.	28	Male	n.d.	n.d.	n.d.	n.d.	S22	14	26	2
7	Control	n.d.	n.a.	30	Female	B	1	n.d.	n.d.	S24	13	29	1
8	Control	n.d.	n.a.	27	Male	n.d.	n.d.	n.d.	n.d.	S26	14	23	1
9	Control	n.d.	n.a.	25	Female	AB	1	n.d.	n.d.	S28	10	14	1
10	Control	n.d.	n.a.	23	Female	B	n.d.	n.d.	n.d.	S30	11	17	1
11	Control	n.d.	n.a.	29	Male	n.d.	n.d.	n.d.	n.d.	S32	21	54	2
12	Control	n.d.	n.a.	23	Male	n.d.	n.d.	n.d.	n.d.	S34	16	53	2
13	Control	n.d.	n.a.	64	Male	n.d.	n.d.	n.d.	n.d.	S38	13	24	1
14	VWD type 1	no	n.a.	32	Female	A	23	42	49	S1	8	13	1
										S3	11	7	1
15	VWD type 1	no	n.a.	66	Female	O	14	38	27	S5	13	19	1
										S7	15	20	1
16	VWD type 1	no	n.a.	39	Female	O	9	48	44	S9	16	35	2
17	VWD type 1	no	n.a.	50	Male	O	24	55	43	S13	17	45	2
18	VWD type 2A	no	n.a.	66	Female	O	14	45	22	S11	9	28	2
										S15	16	26	1
19[a]	VWD type 2B	4022G>C	Arg1341Pro	73	Male	O	12	11	4	S23	17	20	1
20[a]	VWD type 2A	2771G>A	Arg924Gln	88	Male	O	14	15	4	S25	19	25	1
21[a]	VWD type 2A	4120C>T	Arg1374Cys	21	Male	n.d.	10	18	9	S29	14	32	1
22[a]	VWD type 1	421G>A + 6937C>T	Asp141Asn + Arg2313Cys	39	Female	O	12	22	14	S27	13	20	1
										S35	15	21	2
23[a]	VWD type 1	3614G>A	Arg1205His	74	Female	B	12	3	4	S37	12	39	2

Hist., historically; ISTH-BAT, International Society on Thrombosis and Haemostasis Bleeding Assessment Tool; n.a., not applicable; n.d., not determined; VWD, von Willebrand disease; VWF:Act, von Willebrand factor activity; VWF:Ag, von Willebrand factor antigen.

[a] Did not respond to 1-8-deamino-D-arginine vasopressin.

[b] Number of days after inclusion.

[c] From the day of detection to freezing (in days).

30-sample-per-day gradient. Buffer A was composed of 0.1 % formic acid and buffer B of 0.1 % formic acid in acetonitrile (Biosolve). Peptides were ionized and electro-sprayed into the mass spectrometer. Data were acquired in data-independent acquisition parallel accumulation-serial fragmentation mode using an mass spectrometer 1 scan range of 100 to 1700 m/z. Accumulation time was set at 100 milliseconds with a duty cycle of 100%. Mass spectrometer 2 acquisition was performed using 32 pyDIAID [42] optimized mass and ion mobility windows, ranging from 400.2 to 1500.8 m/z and 0.70 to 1.50 1/k0 with a cycle time of 1.80 seconds, respectively. A collision energy of 20.00 eV at 0.6 1/k0 and 59 eV at 1.60 1/k0 was used. Raw mass spectrometry data files were processed using the DIA-neural networks software (Demichev, version 1.8) as previously reported [41]. Data were analyzed using CRAN - R 4.2.3/RStudio. Sample S34 could not be included in the analysis due to technical reasons. Detected proteins were filtered for proteotypic and at least 1 unique peptide per protein. Proteins should be quantified in at least 6 different samples. Label-free quantification (LFQ) values were transformed to a $\log_2$-fold scale. Missing values were imputed by normal distribution (width = 0.3, shift = 1.5), assuming these proteins were close to the detection limit. All LFQ values are available in Supplementary File S3. The analysis script is made available on GitHub (https://github.com/Clotterdam).

2.9 | RNA isolation and quantification with quantitative polymerase chain reaction

All ECFC clones were cultured in 24-well plates at passage 4 and were kept in culture for 5 to 7 days after they reached confluency. Isolation of RNA, synthesis of complementary DNA, and subsequent characterization of ECFCs into clusters by a quantitative polymerase chain reaction (qPCR) gene panel were performed as described previously [36]. Primer sequences of all genes tested are available in Supplementary Table S2. Measurements were analyzed using the comparative Ct method, where GAPDH was used as the housekeeping gene. Results from the qPCR were analyzed using the prcomp function from stats in CRAN - RStudio (version 3.6.2). The script is supplied as Supplementary File S4 (also made available on GitHub; https://github.com/Clotterdam).

2.10 | Statistical analysis

Functional aspects of ECFCs between controls and patient groups were compared with Mann–Whitney U-test (not normally distributed) and unpaired *t*-test with Welch correction (normally distributed). Kruskal–Wallis one-way analysis of variance (ANOVA) was used when comparing >2 groups. Plasma measurements are presented as boxplot with median or as points per ECFC clone, with mean for all others. P value < .05 was considered statistically significant. Data were analyzed using GraphPad Prism 9.3.1 (GraphPad Software) unless otherwise indicated. For proteome analysis, partition around medoids-based clustering was performed using the Cluster package [43], employing a maximum number of clusters of 20 with 100 iterations each. To determine differentially abundant proteins, moderated *t*-tests were performed using Linear Models for Microarray and Omics Data [44,45]. A Benjamini-Hochberg-adjusted $P < .05$ and $\log_2$-fold change >1 was considered significant and relevant. Spearman correlations were calculated using Hmisc [46]. Gene Ontology (GO) term enrichment was performed using the clusterProfiler package [47]; enrichments with a Benjamini-Hochberg-adjusted P value < .05 were considered significant.

3 | RESULTS

3.1 | VWD study population and ECFC isolation

In this study, we aimed to investigate the endothelial compartment as a potential modifier of VWD phenotype by studying ECFCs obtained from 13 healthy controls and from 2 groups of VWD patients in which an endothelial contribution to their disease etiology is plausible: (1) patients without an identified known variant in *VWF*, with a normal response to DDAVP, and (2) patients with VWD with an identified, known variant in *VWF*, who do not respond to DDAVP (Figure 1A). Patients were classified as type 1 (6 patients) or type 2 (4 patients) VWD based on the current VWD diagnostic guideline [48]. Detailed characteristics of the patients and controls are shown in the Table. All functional assay results are shown in Supplementary File S5. Plasma coagulation factor levels (VWF:Act, VWF:Ag, VWF:CB, and FVIII coagulant activity) were determined again at time of inclusion in this study (Figure 1B–E). All measured coagulation factors were significantly lower in DDAVP nonresponders compared with healthy controls. VWF and FVIII levels were also reduced in VWD patients without identified *VWF* variants, but this was only statistically significant for VWF:CB. Compared with historically lowest levels until WiN inclusion and levels measured during the WiN inclusion (12-16 years ago) [32], current levels have partially corrected (Figure 1B–E), which is likely due to an age-dependent increase in plasma VWF levels [23,49–51].

3.2 | ECFC isolation and RNA-based characterization

To study VWD-specific signatures of endothelial cells, we isolated at least 1 ECFC clone from all patients and controls. When multiple clones were isolated per donor, the 2 clones that were first to reach the third passage were taken for this study, which resulted in 15 clones from controls and 14 from patients (Figure 1A). A complete overview of the ECFC clone and donor characteristics is shown in Table. All clones displayed characteristic cobblestone-like endothelial morphology, although with large heterogeneity (Supplementary Figure S1). It is widely recognized that substantial phenotypic heterogeneity can exist between ECFC clones isolated from healthy controls and even from the same individuals [34,40], which can be

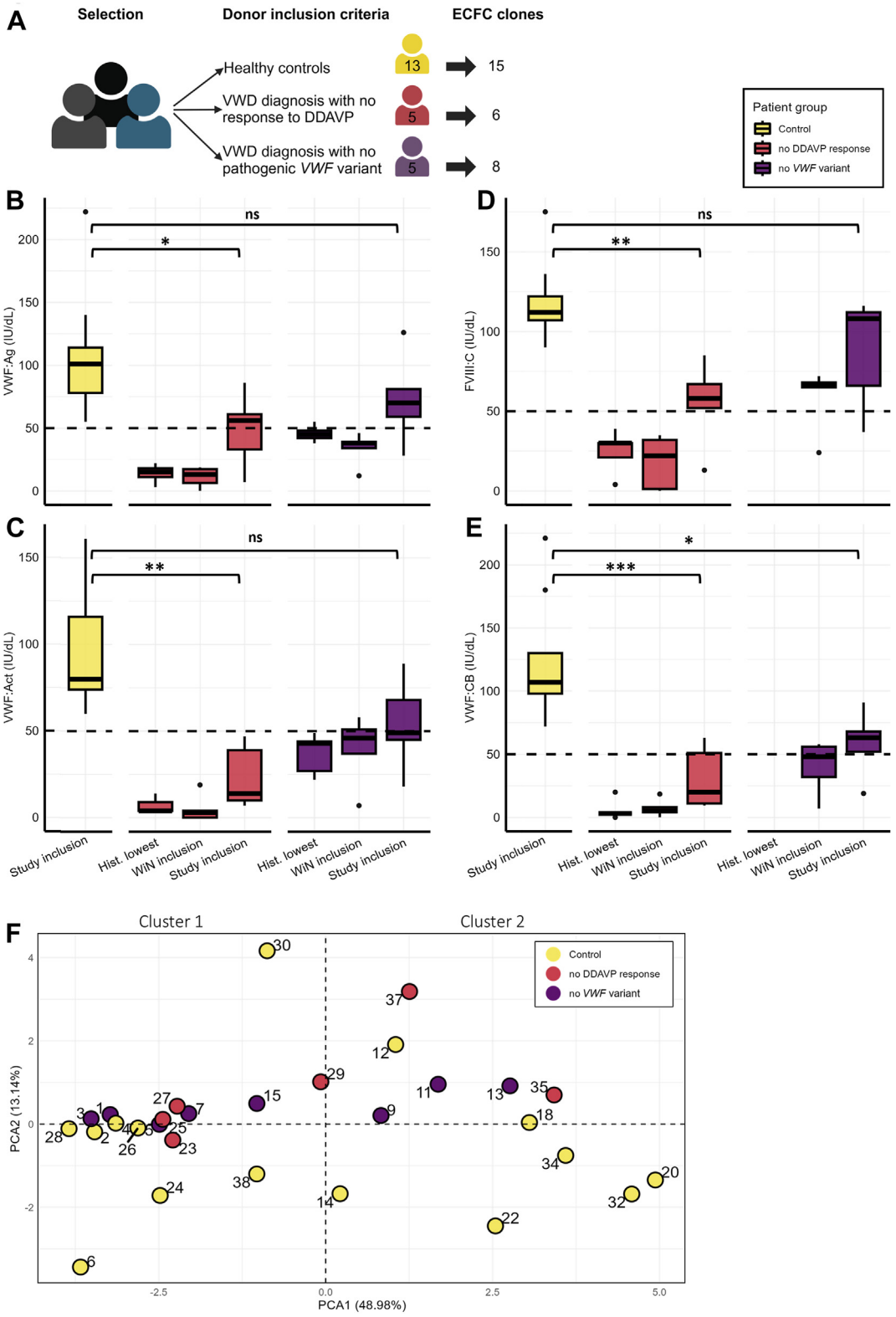

FIGURE 1 Patient and control plasma levels and endothelial colony–forming cell (ECFC) characteristics. (A) Schematic overview of donor inclusion. Boxplots of (B) von Willebrand factor (VWF) antigen (VWF:Ag), (C) VWF activity (VWF:Act), (D) factor VIII coagulant activity (FVIII:C), and (E) VWF collagen binding (VWF:CB) in the plasma of von Willebrand disease (VWD) patients and controls at inclusion in the current study. Furthermore, historically (Hist.) lowest factor levels and levels at time of inclusion in the Willebrand in the Netherlands (WiN) [32] are shown. Statistical analysis was performed by Kruskal–Wallis one-way ANOVA, $^{*}P < .05$, $^{**}P < .01$. Values 1.5 times outside the IQR are shown as black dots. Note that previous VWF activity was measured with different platelet binding assays. In this article, all VWF activity levels are indicated as VWF:Act. (F) Principal component analysis (PCA) plot showing heterogeneity between ECFC clones. All clones on the left of the y-axis were categorized as cluster 1, and clones on the right as cluster 2. Numbers correlate with sample numbers, and color indicates which group the clone belongs to: controls (yellow), VWD patients without 1-8-deamino-D-arginine vasopressin (DDAVP) response (red), and VWD patients without *VWF* variant (purple). IU, International Units; ns, not significant.

explained by the existence of at least 2 discrete transcriptional clusters of ECFCs [36]. We carried out a qPCR-based transcriptional analysis of ECFC clones, as described previously [36] (Supplementary Table S2), which can distinguish between the aforementioned phenotypic clusters of ECFCs. To visualize the variation between clones, we performed principal component analysis (Figure 1F), which revealed large intra and interindividual heterogeneity and allowed us to categorize ECFC clones into cluster 1 and cluster 2 ECFCs through hierarchical clustering (Table). To ensure correct comparison between control and patient ECFCs, we used this categorization in all following assays to compare ECFC clones with clones within their assigned cluster.

3.3 | Morphologic and migratory characterization of ECFCs obtained from VWD patients

Morphology of ECFCs was studied to investigate whether defects in the secretory pathway or abnormal distribution, count, and/or shape of WPBs contribute to the VWD phenotype of the patients. All ECFCs were imaged for VWF, vascular endothelial cadherin, and their nuclei (Figure 2A). Clone S38 is shown as a representative of the control ECFCs and shows typical cigar-shaped WPBs. We observed that 4 (out of 6) ECFCs obtained from 3 patients (out of 5) with DDAVP nonresponse showed retention of VWF in the ER. S29 is shown as representative clone of other ECFCs, S25, S27, and S35, which were confirmed by protein disulfide isomerase staining (Supplementary Figure S2). No uniform morphologic phenotype was seen in patients without identified *VWF* variants, but S11 did display very large cells and small and round WPBs. ECFC characteristics were quantified using an automated image-analysis pipeline developed in CellProfiler [38]. Great variation in cell count, WPB count per cell, organelle eccentricity, and relative distance to the nucleus between all ECFCs was observed (Figure 2B–E), as was also shown previously in healthy controls [36,38]. Between patient groups and controls, only mean organelle eccentricity was found to be significantly lower in cluster 1 ECFCs of patients without DDAVP response. This effect was primarily attributable to the ECFCs that showed ER retention (clones S25, S27, S29, and S35), which, on average, had lower organelle eccentricity (mean ± SD, 0.637 ± 0.015 vs control 0.721 ± 0.039) and WPB count per cell (35.97 ± 24.20 vs control 132.30 ± 27.60). Together, these data show a phenotype in ECFCs of some DDAVP nonresponders that results in retention of VWF in the ER, which could reduce its availability for stimulus-induced release of VWF from WPBs.

It has been shown that VWF plays a role in migration, proliferation, and angiogenesis of endothelial cells [52] and that some ECFCs obtained from type 1 and 2 VWD patients have lower directionality in wound healing assays [53]. Therefore, we also analyzed the migration behavior of all ECFCs using a scratch wound migration assay (Supplementary Figure S3A). We observed that cluster 1 DDAVP nonresponder ECFCs had a slower closing speed compared with control ECFCs, while cluster 2 ECFCs from DDAVP nonresponders closed the scratch faster than controls (Supplementary Figure S3B). No significant differences were observed for speed of movement, X trajectory, and linearity (Supplementary Figure S3C). However, samples S25, S27, and S29 in cluster 1 did show markedly decreased X trajectory. This suggests that ECs with observed ER retention and decreased VWF levels also have implicated migratory processes.

3.4 | Impaired synthesis and secretion upon stimulation of patient ECFCs

We investigated whether production of VWF and secretory capabilities of the ECFCs may clarify the low VWF levels or lack of response to DDAVP. We measured basal VWF secretion over 24 hours (Figure 3A), intracellular VWF content in the lysate (Figure 3B), and regulated secretion of VWF following Ca^{2+}- (histamine) and cyclic adenosine monophosphate-mediated (epinephrine) stimulation (Figure 3C, D). Cluster 1 ECFCs from DDAVP nonresponders had significantly lower basal VWF release (Figure 3A) and lower intracellular VWF content (Figure 3B) than control ECFCs, while ECFCs from patients with no *VWF* variant (but who were responsive to DDAVP) did not differ from controls. Cluster 1 DDAVP nonresponder ECFCs also showed a trend toward lower VWF secretory response upon histamine and epinephrine stimulation (Figure 3C, D), whereas ECFCs from patients without identified *VWF* variants responded comparably to control ECFCs. We next correlated VWF synthesis and secretion in ECFCs with plasma VWF levels (Figure 3E–H). ECFCs in cluster 1 showed positive correlations between plasma VWF:Ag levels and basal VWF secretion (Figure 3E), VWF synthesis (Figure 3F), as well as histamine- (Figure 3G) and epinephrine-stimulated secretion (Figure 3H), while there were no such correlations in cluster 2 ECFCs. This suggests that cluster 1 ECFCs are a good representative of VWF synthesis and secretion in the vessels of the patients.

3.5 | VWD does not drive disease-specific proteomic differences

Next, we investigated whether we could find differences in protein abundance in ECFCs obtained from VWD patients. Therefore, we performed unbiased proteomics on 28 ECFC clones using a bottom-up LFQ mass spectrometry workflow (Figure 4A). On average, 8349 proteins were quantified per sample (Supplementary Figure S4A) with an overall high correlation (Supplementary Figure S4B). Based on principal component analysis, we did not observe a clear distinction between controls and the 2 VWD patient categories (Figure 4B). Partition around medoids clustering of the proteomes identified 3 ECFC clusters (A, B, and C; Figure 4C), of which clusters A and B partially overlapped with the annotation based on the qPCR panel (Figure 4D). Statistical analysis comparing ECFCs obtained from healthy controls with ECFCs obtained from VWD patient groups (LFC >1; $P < .05$) did not reveal differentially abundant proteins (Figure 4E). To remove interference from different ECFC types, testing was also performed within the different clusters based on the proteome data (Figure 4F) and qPCR panel (Figure 4G), but none showed

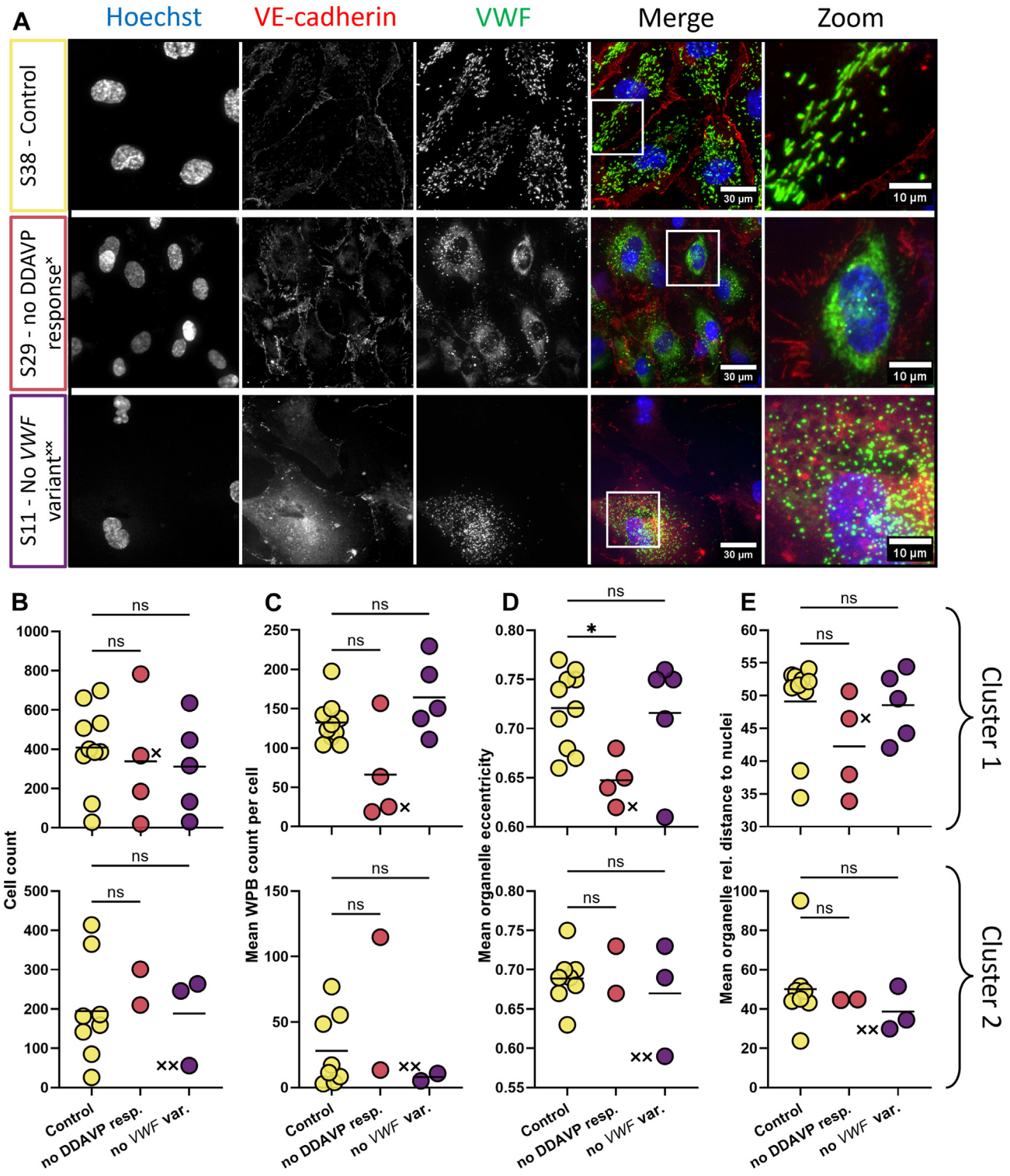

FIGURE 2 Morphologic differences of endothelial colony–forming cells (ECFCs) obtained from von Willebrand disease patients. Phenotypic profiling of all ECFCs was done using tile scans (1123261 µm^2). ECFC clones were analyzed per cluster and stained with Hoechst (blue) and antibodies against vascular endothelial cadherin (VE-cadherin; red) and von Willebrand factor (VWF; green). (A) Representative confocal images of a control ECFC clone (top–S38), a patient with retention of VWF in the endoplasmic reticulum (middle–S29), and a patient ECFC with round Weibel–Palade bodies (WPBs; bottom–S11). The scale bar represents 30 µm. The white box indicates the area that is enlarged by 3× of the merged image (scale bar represents 10 µm). Images were taken with a 63× objective. (B) Cell count per surface area of the tile scan. (C) Mean WPB count per cell per ECFC clone. (D) Mean eccentricity of WPBs per ECFC clone. (E) Distance of the WPBs to the nucleus relative to their position in the cell in percentage. S29 and S11 values are indicated by x and xx, respectively, in B–E. Values per ECFC clone are shown, and the line shows the mean. Kruskal–Wallis one-way ANOVA was performed; *$P < .05$. DDAVP, 1-8-deamino-D-arginine vasopressin; ns, not significant; resp., responder; var., variant.

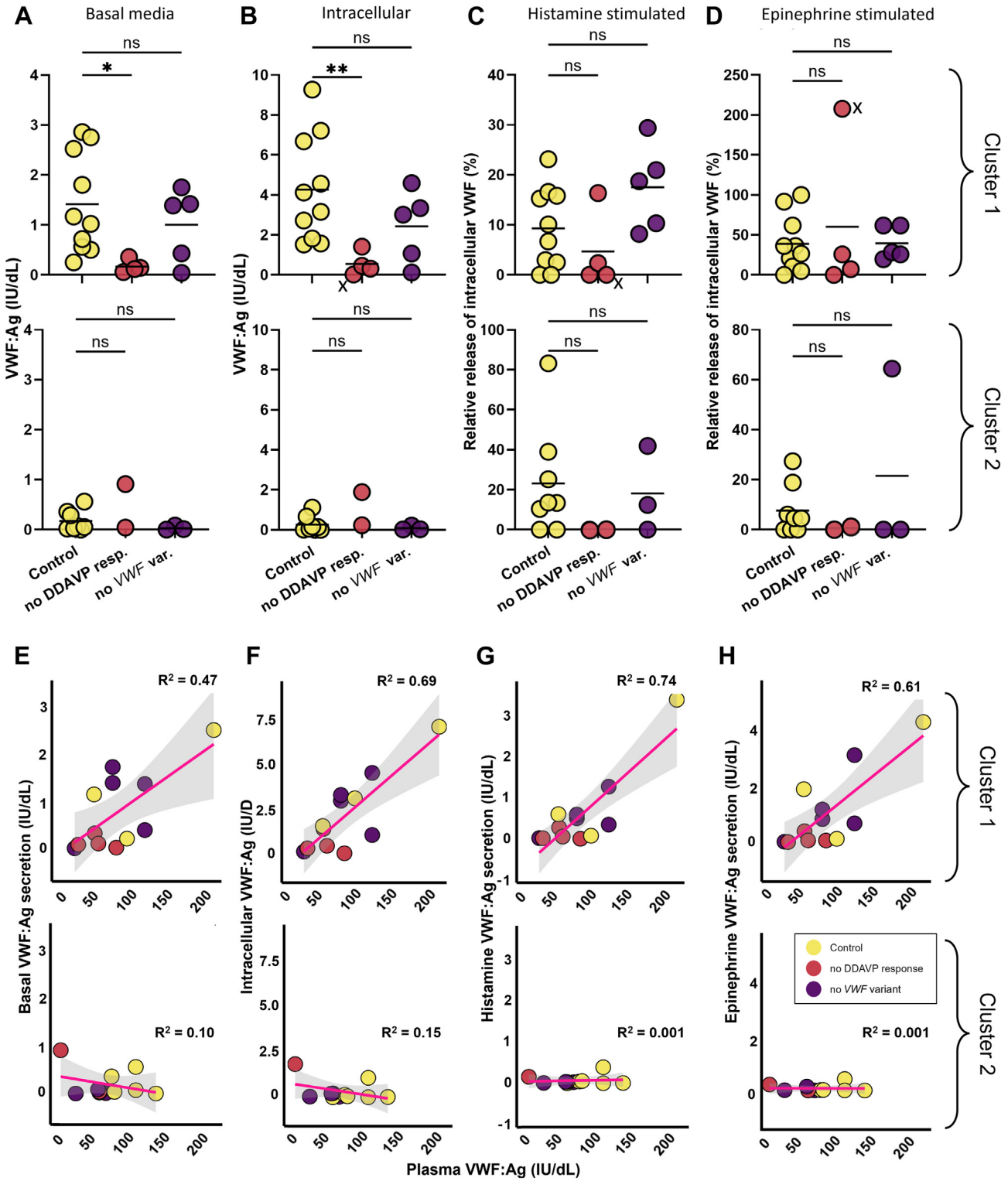

FIGURE 3 von Willebrand factor (VWF) production and secretion are lower in patient endothelial colony–forming cells (ECFCs). ECFCs were grown in culture until confluent and then stimulated by histamine and epinephrine + IBMX to secrete VWF. VWF antigen (VWF:Ag; International Units [IU]/dL) levels as measured by enzyme-linked immunosorbent assay are shown per ECFC clone. (A) VWF levels are secreted in media during 24 hours of culture of ECFCs preceding the stimulation. (B) VWF levels in the lysates of unstimulated cells (dimethyl sulfoxide exposure only). (C) Secretion of VWF after 1 hour of stimulation as a percentage of the total amount of VWF in the cell. Calculated as the released VWF:Ag in media minus VWF:Ag released without stimulant (dimethyl sulfoxide) divided by the total amount of VWF in the cell (the lysate of the unstimulated cells). If stimulated release was not higher than the negative control, a value of 0 was noted. Plasma VWF:Ag measurements were correlated to the basal release levels of VWF:Ag by the (E) ECFCs, (F) in the lysate, (G) secreted after histamine stimulation, and (H) secreted after epinephrine + IBMX stimulation. Statistical analysis was performed by Kruskal–Wallis one-way ANOVA, $^{*}P < .05$, $^{**}P < .01$. R^2 was calculated by linear regression. DDAVP, 1-8-deamino-D-arginine vasopressin; ns, not significant; resp., responder; var., variant. The sample marked by x indicates a DDAVP nonresponder ECFC in cluster 1, which had intracellular VWF levels close to the detection limit of the ELISA. Due to the low levels, the relative secretion is incorrectly high.

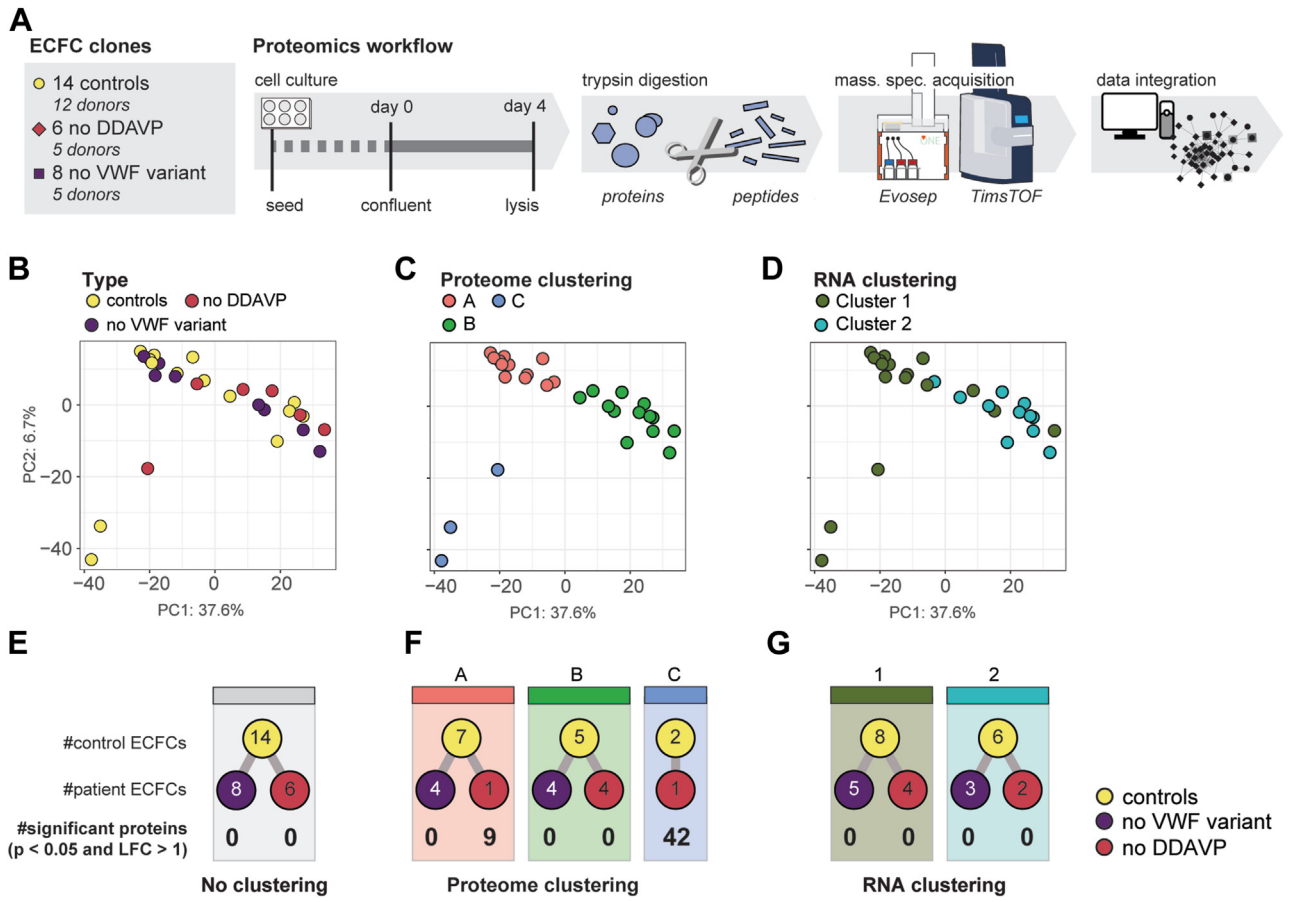

FIGURE 4 von Willebrand disease does not drive disease-specific proteomic differences. (A) Schematic overview of proteomics workflow. Principal component (PC) analysis of proteomes across PC1 and PC2, colored based on (B) disease type, (C) proteomics-based clustering, and (D) quantitative polymerase chain reaction-based division. Overview of samples and significantly regulated proteins (*t*-test, $P < .05$ and $\log_2$-fold change [LFC] >1) between (E) disease type vs controls, (F) disease type vs control per proteome cluster, and (G) disease type vs controls per quantitative polymerase chain reaction-based distinction. DDAVP, 1-8-deamino-D-arginine vasopressin; ECFC, endothelial colony–forming cell; mass. spec., mass spectrometry; VWF, von Willebrand factor.

group-specific differences. A comparison of individual patient ECFC clones vs controls within the proteomics clusters did reveal clone-specific alterations (Supplementary Figure S4C). However, the observed heterogeneity in ECFC clones obtained from the same donor (Supplementary Figure S4D), combined with marginal overlap in regulated proteins between ECFC clones from same VWD donor (Supplementary Figure S4E), hampered interpretation of donor-specific differences. Finally, we plotted the VWF coverage across all samples, which mainly corresponded to the heterogeneity in VWF levels across ECFC clones (Supplementary Figure S5A). In one of the patient-derived ECFCs, the Arg1374Cys variation was detected (Supplementary Figure S5B). Taken together, this highlights the challenge of dissecting VWD-specific defects in an individual patient.

3.6 | Proteomic signatures of heterogeneous ECFC phenotypes

To further investigate endothelial heterogeneity in the context of VWD, we explored the differences that drive separation into clusters A, B, and C (Figure 4C). On a morphologic level, cluster A contained ECFCs with hallmark cobblestone morphology, while cluster B contained cells with a more inflamed and mesenchymal-like phenotype (Figure 5A), in agreement with qPCR segregation. Among the proteins driving the most variation between proteomic clusters A and B were ALDH1A1, CLU, and VWF (increased abundance in cluster A), and TGFBI, CD44, and TAGLN (increased abundance in cluster B), which were previously described as separating cobblestone-mesenchymal phenotypes by RNA sequencing [34] (Figure 5B, C). In total, 316 of 451 significantly different proteins between groups A and B were also identified in that study at transcript level (Supplementary Figure S6A, B). GO enrichment indicated that cluster A was enriched for metabolism and Golgi-system activity, while cluster B was enriched for extracellular matrix components such as collagens (COL8A1), fibulin (FBLN1), and fibronectin (Figure 5D and Supplementary Figure S6C). Moreover, cell type-specific enrichment analysis of the differentially expressed proteins between cluster A and B ECFCs using WebCSEA [54] showed that cluster A was enriched predominantly for ECs, while cluster B was enriched for connective tissue cells such as fibroblasts, stromal cells, and smooth muscle cells (Supplementary Figure S6D).

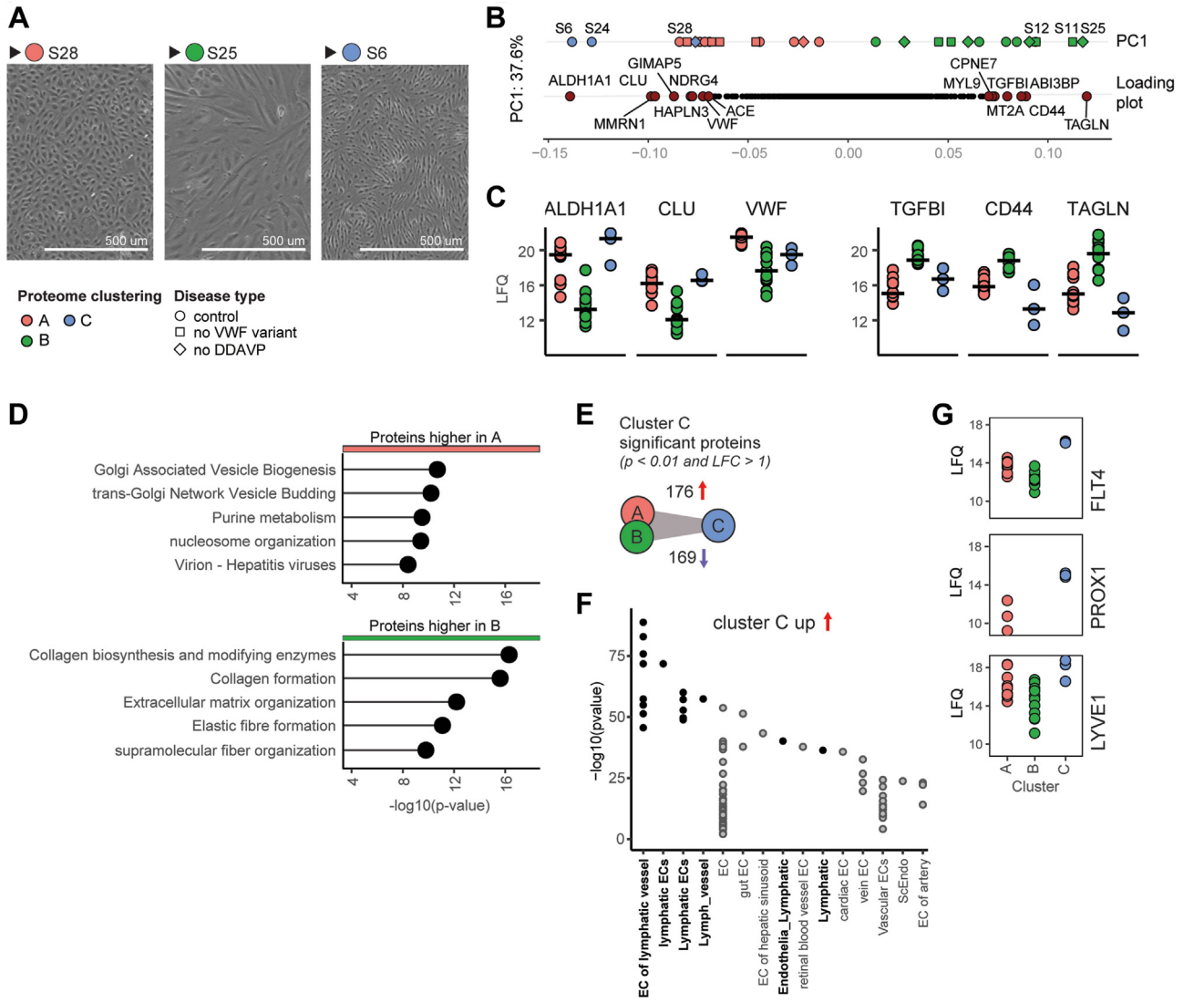

FIGURE 5 Proteomic signatures of heterogeneous endothelial colony–forming cell phenotypes. (A) Brightfield images of hallmark endothelial colony–forming cell clones per proteomic cluster; scale bar indicates 500 μm. (B) Distribution of samples and loading plot across principal component (PC) 1; shape indicates disease type (control–circle; no 1-8-deamino-D-arginine vasopressin [DDAVP]–diamond; no von Willebrand factor [VWF] variant—square). Highest positive and negative separating proteins in the loading plot are highlighted in red and labeled. (C) Dot plots of protein label-free quantification (LFQ) values with high positive and negative separation across PC1. (D) Gene Ontology enrichment of proteins that are differentially abundant between clusters A and B. Colors indicate enrichment of proteins higher in A (red) and higher in B (green). (E) Number of up- and downregulated proteins (*t*-test, *P* value < .05; $\log_2$-fold change [LFC] >1) in cluster C vs clusters A and B. (F) Top 15 WebCSEA enriched endothelial cell (EC) subtype terms of upregulated proteins in group C. Colors indicate lymphatic EC terms (black) and other EC terms (gray). (G) Dot plots of lymphatic protein LFQ values.

These findings further support the mesenchymal traits of this group of ECFCs. Interestingly, cells in cluster C showed a unique phenotype of spindle-like ECs that diverged from clusters A and B. The variation across principal component 2, which mostly separated cluster C, was driven by RELN, TIMP3, and CEACAM1, among others (Supplementary Figure S6E, F). In total, 345 proteins were differentially abundant in cluster C compared with clusters A and B (LFC >1; *P* < .05; Figure 5E). WebCSEA [54] cell-type enrichment of these proteins had the highest enrichment for lymphatic ECs (Figure 5F). Moreover, lymphatic markers PROX1, VEGFR3 (FLT4), and, to a lesser extent [55–57], were all more abundant in cluster C ECFCs (Figure 5G), suggesting these clones are of lymphatic endothelial lineage.

3.7 | Combined data integration to decipher proteomic profiles in the context of VWF

To investigate proteomic profiles in the context of VWF across a heterogeneous ECFC population, we integrated VWF secretion, qPCR cluster profiles, and morphologic and functional data with protein expression profiles. Correlation analysis revealed that abundance of

an extensive network of proteins (N = 2173) was associated with a functional or cell biological outcome (Spearman correlation coefficient > .7; Supplementary Figure S7A). As expected, VWF:Ag levels in lysates and secreted VWF measured by ELISA correlated highly with the proteome VWF LFQ measurements (Spearman correlation > .85; Supplementary Figure S7B). VWF LFQ, VWF:Ag, and secreted VWF levels also correlated positively with cell and WPB counts, and inversely with cell area (Supplementary Figure S7A). Proteins positively correlated with histamine-induced VWF secretion (n = 791), enriched predominantly for the GO biological process term "RNA processing," and proteins inversely correlated (n = 550) with biological process enriched for "Endomembrane system" (Figure 6A). To specifically look for proteins associated with the VWF exocytosis machinery and WPBs, we highlighted known and putative WPB interactor proteins [2] and found that important adaptors in VWF release were positively correlated with increased VWF release, such as RAB27A, RAB3D, and SYTL4 [58–60], while others, such as GBF1, which is important in ER-Golgi trafficking of VWF, correlated negatively (Figure 6B). Of these proteins, only RAB3D also positively correlated with WPB count per cell (Figure 6C). This suggests that, while both RAB3D and RAB27A are important in WPB release, RAB3D also functions in managing WPBs in steady state. Surprisingly, IGFBP7, a protein known to be present in WPBs [61], was lower in abundance when more WPBs were present per cell (Figure 6D). Moreover, 18 mitochondrial proteins correlated positively with WPB count. Interestingly, several of these proteins, particularly those involved in protein import into mitochondria (eg, AGK, TOMM70, and small TIMs [62]), showed high correlation with WPB count, while other mitochondrial proteins that they are known to interact (TOMM40 and TIMM22) did not (Supplementary Figure S7C). The interaction between mitochondria and WPBs has been indicated to facilitate WPB maturation [63], suggesting a potential function of these proteins in the life cycle of WPBs. Finally, correlating proteins to organelle eccentricity, which is a proxy for ER retention, was limited. However, several members of the vacuolar-ATPase (ATP6V-B1, -E1, -G1, and -H1) negatively correlated with organelle eccentricity (Figure 6E). Counterintuitively, although v-ATPase proton pump is required for the maturation of WPBs [61,64,65], our analysis showed that higher levels of this protein correlated with round WPBs (Figure 6F).

4 | DISCUSSION

ECFCs have been used to study biological processes in endothelial cells and elucidate the pathogenic mechanisms of various diseases [29,30,53]. There is a lot of variability in bleeding phenotype in patients with VWD [4], and it is hypothesized that other modifiers cause the low levels of VWF and associated bleeding [25] or perhaps nonresponse to DDAVP treatment. Therefore, in this study, we used ECFCs to attempt to unravel those mechanisms. Patients were previously diagnosed with VWD based on reduced levels of plasma VWF:Ag and VWF:Act, which correlated with low levels of produced and secreted VWF by ECFCs. Furthermore, we observed retention of VWF in the ER, which was connected with very low levels of secreted VWF. Proteomic characterization of the ECFC clones yielded distinct clusters of ECFC clones that were not dependent on patient groups. Proteomic clustering overlapped with RNA-based clustering and yielded a third cluster in this study, which seems to be of lymphatic endothelial lineage. Finally, comparing functional outcomes to proteomics, we observed that VWF levels and WPB count per cell correlated inversely with cell area, and regulated secretion of VWF and WPB count in ECFCs was correlated with various secretory machinery components. Protein regulation showed strong enrichment of DNA and messenger RNA processing in cells with high VWF levels and a smaller cell area.

Despite the advantages of ECFCs, considerable phenotypic heterogeneity has been observed [34,36,40], which is influenced by day of initial appearance of ECFCs [34], passaging [66], and duration in culture [67,68]. Interestingly, the proteomic heterogeneity between clones was remarkably similar to the transcriptomic differences observed previously [36], even though different ECFCs, cultured in separate laboratories, were used. Three hundred sixteen of 451 significantly different proteins between groups A and B were previously measured by RNA sequencing [36]. This large overlap indicates that ECFCs maintain similar patterns in both protein and RNA expression levels. Furthermore, endothelial-to-mesenchymal–associated proteins, TGFBI, TGFB2, and BMP2 [69], were also found to be significantly different at the proteome level. The overlap between the transcriptome and the proteome suggests that the characterization of ECFCs could also be performed at the protein level, which is comparable with qPCR panel we have used, and could lead to better characterization if combined.

While the origin of circulating ECFCs is uncertain, the heterogeneity we observed between clones resembles the differences in expression profiles between endothelial cells from distinct vascular beds [41,70]. The proteomic signature showed a distinct cluster enriched for ECs of lymphatic endothelial lineage. These cells were visually smaller and more spindle-like compared with other ECFC clones, and they had higher protein levels of transcription factors PROX1 [71] and CEACAM1, which are important in the formation of new lymphatic vessels [72]. Whether the observed ECFCs respond differently to external stimuli remains to be elucidated, but it provides an interesting avenue to investigate vascular bed-related differences using ECFCs.

We hypothesized that unexplained nonresponse to DDAVP could be caused by modifiers outside of *VWF*. ECFCs that showed retention of VWF in the ER were all obtained from DDAVP nonresponsive patients who carried a *VWF* variant. The p.Arg924Gln variant (S25) is associated with reduced VWF and FVIII levels [73], but ER retention in previous studies has not been confirmed through any staining. S27 and S35 (from the same patient) carry p.Asp141Asn and p.Arg2313Cys, respectively. The variant p.Asp141Asn has been shown to cause ER retention in transfected human embryonic kidney cells [74], which we have now confirmed in ECFCs carrying this variant. Finally, p.Arg1374Cys (S29) is still disputed as causing either VWD type 2A or 2M [75], but we show here that this variant is accompanied by

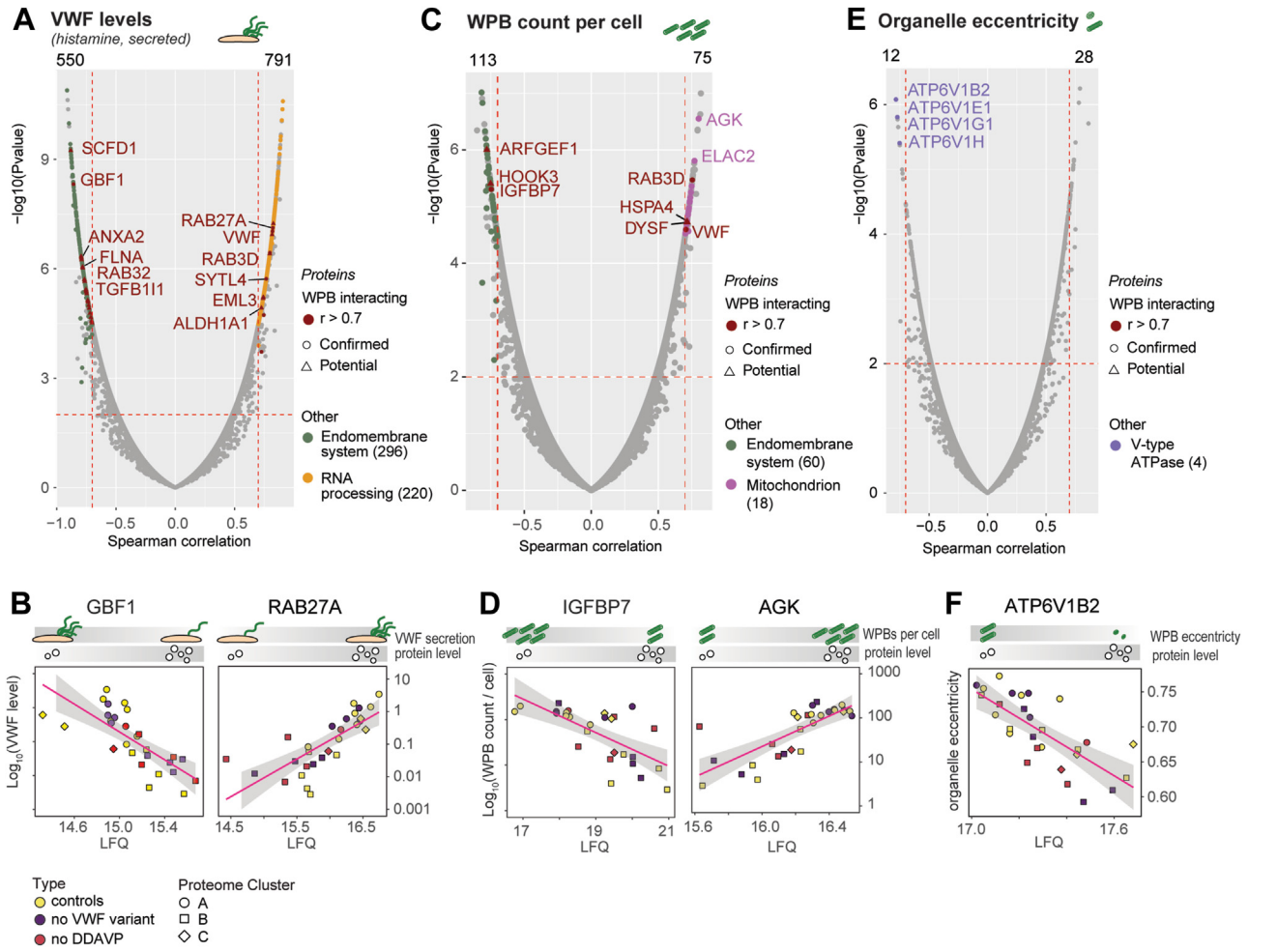

FIGURE 6 Proteomic and functional data integration. (A) Spearman correlation plot of histamine-induced secreted von Willebrand factor (VWF) levels with protein label-free quantification (LFQ) levels, and (B) protein correlations of interest. (C) Spearman correlation plot of Weibel–Palade body (WPB) count per cell with protein LFQ levels, and (D) protein correlations of interest. (E) Spearman correlation plot of organelle eccentricity with protein LFQ levels, and (F) protein correlations of interest. For all Spearman correlation plots, correlations > .7 and *P* values < .01 are indicated by dotted red lines. Total number of proteins above cutoffs is indicated at the top of graph. WPB-interacting proteins are indicated in red. Major enriched Gene Ontology terms per functional output and number of proteins per term are shown. DDAVP, 1-8-deamino-D-arginine vasopressin.

significant retention within the ER. Collectively, the retention of VWF in the ER, which would prevent it from progressing to WPBs from where it can be released via basal and stimulus-induced secretion, appears to be a common mechanism in VWD, which could explain the lower circulating levels of VWF and the subsequent nonresponse to DDAVP.

In this study, we show that circulating VWF plasma levels correlate with the amount of VWF contained in ECFCs and the amount of VWF that is released from ECFCs upon stimulated secretion, which confirms the relevance of ECFCs as *ex vivo* cell models for VWF secretion *in vivo*. Moreover, we show that protein levels of various secretion machinery proteins, such as RAB27A, RAB3D, VWF, and SYTL4, were significantly correlated with the stimulated release of VWF and WPB count. Taken together, this suggests that the exocytotic machinery that is recruited to WPBs is a determinant of circulating VWF, which is in line with previous findings from genome-wide association studies that identified components of the secretory pathway, such as *STX2* and *STXBP5*, as determinants of VWF plasma levels [76–78]. Interestingly, the correlation between plasma VWF:Ag and ECFC VWF levels (intracellular and released after stimulus) was only observed in cluster 1 cobblestone ECFCs and not in cluster 2 mesenchymal/inflamed-like ECFCs. This raises the question whether cluster 2 ECFCs are representative of the endothelial compartment that is responsible for production of VWF that circulates in plasma and underscores the intricate connection between VWF and inflammation [79].

A limitation of this study was that patient characteristics were very diverse, and despite ECFC matching, no common cause for the VWD phenotype was found. ECFC variation between groups was not representative of individual patient heterogeneity. Therefore, we focused on patient-specific qualitative findings rather than quantitative results. Our findings remain to be validated in a different setting

or larger cohort to confirm whether these are patient-specific differences that contribute to the bleeding phenotype or arise from ECFC variation. Furthermore, other functional aspects, like angiogenesis, proliferation, and apoptosis, were not included in this study. Analysis of ECFCs from patients with a bleeding disorder of unknown cause, especially those with gastrointestinal bleeding, might benefit from these assays. Moreover, as bleeding is mediated through the interplay of different cells, incorporation of multiple cell types, such as platelets and leukocytes, or the addition of shear stress in a flow model, might boost future studies in unraveling VWD bleeding phenotypes.

Finally, to our knowledge, this study is the first to examine a large panel of ECFCs of both healthy and VWD donors through extensive characterization by both functional assays and proteomics. As such, it highlights the current opportunities and challenges in using ECFCs as a model to study WPB-specific mechanisms and provides a broad EC-wide picture of the molecular regulation of WPB machinery and its outcomes.

APPENDIX

List of SYMPHONY members

Amsterdam, Noord Holland, the Netherlands: Martijn Brands, Sjoerd Koopman, Laura Bukkems, Michael Cloesmeijer, Alexander Janssen, Karin Fijnvandraat, Samantha Gouw, Ron Mathôt, Lotte Haverman, Emile van den Akker, Maartje van den Biggelaar, Masja de Haas, Sander Meijer, Jan Voorberg, Jessica Del Castillo Alferez, Huan Zhang, and Johan Boender. Den Haag, Zuid Holland, the Netherlands: Stephan Meijer. Groningen, Groningen, the Netherlands: Karina Meijer. Hoofddorp, Noord Holland, the Netherlands: Sean de Jong. Leiden, Zuid Holland, the Netherlands: Geertje Goedhart, Anske van der Bom, Mettine Bos, Jeroen Eikenboom, Felix van der Meer, and Sebastiaan Laan. Nijmegen, Gelderland, the Netherlands: Saskia Schols. Rotterdam, Zuid Holland, the Netherlands: Ruben Bierings, Lex Burdorf, Marjon Cnossen, Jan Hazelzet, Elise Huisman, Marieke Kruip, Frank Leebeek, Nikki van Leeuwen, Hester Lingsma, Moniek de Maat, Iris van Moort, Suzanne Polinder, Simone Reitsma, Eliza Roest, Ryanne Arisz, Lorenzo Romano, Wala Al Arashi, Shannon van Hoorn, Tine Goedhart, Caroline Mussert, Diaz Prameyllawati, and Carin Uyl. Utrecht, Utrecht, the Netherlands: Nathalie Jansen, Kathelijn Fischer, Hans Kristian Ploos van Amstel, Rolf Urbanus, Minka Zivkovic, Annelien Bredenoord, Rieke van der Graaf, Lieke Baas, Roger Schutgens, and Mariëtte Driessens.

ACKNOWLEDGMENTS

The SYMPHONY consortium, which aims to orchestrate personalized treatment in patients with bleeding disorders, is a unique collaboration between patients, health care professionals, and translational and fundamental researchers specializing in inherited bleeding disorders, as well as experts from multiple disciplines [80]. It aims to identify the best treatment choice for each individual based on bleeding phenotype. To achieve this goal, work packages (WPs) have been organized according to 3 themes (eg, Diagnostics [WPs 3 and 4], Treatment [WPs 5-9], and Fundamental Research [WPs 10-12]). Principal investigator: M. H. Cnossen; project manager: S. H. Reitsma.

Beneficiaries of the SYMPHONY consortium: Erasmus University Medical Center–Sophia Children's Hospital, project leadership and coordination; Sanquin Diagnostics; Sanquin Research; Amsterdam University Medical Centers; University Medical Center Groningen; University Medical Center Utrecht; Leiden University Medical Center; Radboud University Medical Center; Netherlands Society of Hemophilia Patients (NVHP); Netherlands Society for Thrombosis and Hemostasis (NVTH); Bayer B.V., CSL Behring B.V., Swedish Orphan Biovitrum (Belgium) BVBA/SPRL.

Funding by SYMPHONY: NWO-NWA.1160.18.038 (received by S.N.J.L., I.v.M., R.B., and J.E.), and Landsteiner Foundation for Blood Transfusion Research, Grant Number: 1707 (received by R.B.).

We would like to acknowledge Suzan de Boer, Yvonne Jongejan, Noa Linthorst, Isabel Bär, Sophie Hordijk, Calvin van Kwawegen, and Ferdows Atiq for their collaboration and assistance with patient selection, inclusion, and endothelial colony–forming cell isolation and culture.

AUTHOR CONTRIBUTIONS

S.N.J.L., R.J.D., S.G., and P.E.B. performed research; S.N.J.L., R.J.D., and S.G. analyzed data; S.N.J.L., R.J.D., I.v.M., S.G., M.v.d.B., F.W.G.L., P.E.B., R.B., and J.E. designed the research, wrote the paper, and provided feedback on the manuscript.

DECLARATION OF COMPETING INTERESTS

The Willebrand in the Netherlands study was supported by the Dutch Haemophilia Foundation, the Erasmus University Medical Center, CSL Behring, and Takeda (funding obtained by F.W.G.L.). F.W.G.L. is a consultant for CSL Behring, BioMarin, and Takeda, with the fees going to the university. J.E. received research funding from CSL Behring, with funds going to the university. All other authors declare no conflicts of interest.

DATA AVAILABILITY

All data files are available in a repository https://figshare.com/projects/Data_repository_-_Von_Willebrand_disease-specific_defects_and_proteomic_signatures_in_endothelial_colony_forming_cells/229449

Proteome raw and search files have been deposited in the ProteomeXchange Consortium (http://proteomecentral.proteomexchange.org/cgi/GetDataset) via the PRIDE partner repository with the dataset identifier *PXD055124*.

ORCID

Sebastiaan N.J. Laan https://orcid.org/0000-0001-9206-8712

REFERENCES

[1] Valentijn KM, Sadler JE, Valentijn JA, Voorberg J, Eikenboom J. Functional architecture of Weibel–Palade bodies. *Blood*. 2011;117:5033–43.

[2] Hordijk S, Carter T, Bierings R. A new look at an old body: molecular determinants of Weibel–Palade body composition and von Willebrand factor exocytosis. *J Thromb Haemost*. 2024;22:1290–303.

[3] Schillemans M, Karampini E, Kat M, Bierings R. Exocytosis of Weibel–Palade bodies: how to unpack a vascular emergency kit. *J Thromb Haemost*. 2019;17:6–18.

[4] Leebeek FW, Eikenboom JC. Von Willebrand's disease. *N Engl J Med*. 2016;375:2067–80.

[5] Murray EW, Lillicrap D. von Willebrand disease: pathogenesis, classification, and management. *Transfus Med Rev*. 1996;10:93–110.

[6] Castaman G. How I treat von Willebrand disease. *Thromb Res*. 2020;196:618–25.

[7] Atiq F, Heijdra J, Snijders F, Boender J, Kempers E, van Heerde WL, Maas DPMSM, Krouwel S, Schoormans SC, de Meris J, Schols SEM, van Galen KPM, van der Bom JG, Cnossen MH, Meijer K, Fijnvandraat K, Eikenboom J, Leebeek FWG. Desmopressin response depends on the presence and type of genetic variants in patients with type 1 and type 2 von Willebrand disease. *Blood Adv*. 2022;6:5317–26.

[8] Biguzzi E, Siboni SM, Peyvandi F. Acquired Von Willebrand syndrome and response to desmopressin. *Haemophilia*. 2018;24:e25–8.

[9] Castaman G, Lethagen S, Federici AB, Tosetto A, Goodeve A, Budde U, Batlle J, Meyer D, Mazurier C, Fressinaud E, Goudemand J, Eikenboom J, Schneppenheim R, Ingerslev J, Vorlova Z, Habart D, Holmberg L, Pasi J, Hill F, Peake I, et al. Response to desmopressin is influenced by the genotype and phenotype in type 1 von Willebrand disease (VWD): results from the European Study MCMDM-1VWD. *Blood*. 2008;111:3531–9.

[10] Castaman G, Mancuso ME, Giacomelli SH, Tosetto A, Santagostino E, Mannucci PM, Rodeghiero F. Molecular and phenotypic determinants of the response to desmopressin in adult patients with mild hemophilia A. *J Thromb Haemost*. 2009;7:1824–31.

[11] Castaman G, Tosetto A, Eikenboom JC, Rodeghiero F. Blood group significantly influences von Willebrand factor increase and half-life after desmopressin in von Willebrand disease Vicenza. *J Thromb Haemost*. 2010;8:2078–80.

[12] Castaman G, Rodeghiero F. No influence of blood group on the responsiveness to desmopressin in type I "platelet normal" von Willebrand's disease. *Thromb Haemost*. 1995;73:551–2.

[13] Di Perna C, Riccardi F, Franchini M, Rivolta GF, Pattacini C, Tagliaferri A. Clinical efficacy and determinants of response to treatment with desmopressin in mild hemophilia A. *Semin Thromb Hemost*. 2013;39:732–9.

[14] Lethagen S, Egervall K, Berntorp E, Bengtsson B. The administration of desmopressin by nasal spray: a dose-determination study in patients with mild haemophilia A or von Willebrand's disease. *Haemophilia*. 1995;1:97–102.

[15] Nance D, Fletcher SN, Bolgiano DC, Thompson AR, Josephson NC, Konkle BA. Factor VIII mutation and desmopressin-responsiveness in 62 patients with mild haemophilia A. *Haemophilia*. 2013;19:720–6.

[16] Revel–Vilk S, Schmugge M, Carcao MD, Blanchette P, Rand ML, Blanchette VS. Desmopressin (DDAVP) responsiveness in children with von Willebrand disease. *J Pediatr Hematol Oncol*. 2003;25:874–9.

[17] Revel–Vilk S, Blanchette VS, Sparling C, Stain AM, Carcao MD. DDAVP challenge tests in boys with mild/moderate haemophilia A. *Br J Haematol*. 2002;117:947–51.

[18] Seary ME, Feldman D, Carcao MD. DDAVP responsiveness in children with mild or moderate haemophilia A correlates with age, endogenous FVIII:C level and with haemophilic genotype. *Haemophilia*. 2012;18:50–5.

[19] Sharthkumar A, Greist A, Di Paola J, Winay J, Roberson C, Heiman M, Herbert S, Parameswaran R, Shapiro A. Biologic response to subcutaneous and intranasal therapy with desmopressin in a large Amish kindred with type 2M von Willebrand disease. *Haemophilia*. 2008;14:539–48.

[20] Stoof SC, Sanders YV, Petrij F, Cnossen MH, de Maat MP, Leebeek FW, Kruip MJ. Response to desmopressin is strongly dependent on F8 gene mutation type in mild and moderate haemophilia A. *Thromb Haemost*. 2013;109:440–9.

[21] de Jong A, Eikenboom J. Von Willebrand disease mutation spectrum and associated mutation mechanisms. *Thromb Res*. 2017;159:65–75.

[22] James PD, Notley C, Hegadorn C, Leggo J, Tuttle A, Tinlin S, Brown C, Andrews C, Labelle A, Chirinian Y, O'Brien L, Othman M, Rivard G, Rapson D, Hough C, Lillicrap D. The mutational spectrum of type 1 von Willebrand disease: results from a Canadian cohort study. *Blood*. 2007;109:145–54.

[23] Lavin M, Aguila S, Schneppenheim S, Dalton N, Jones KL, O'Sullivan JM, O'Connell NM, Ryan K, White B, Byrne M, Rafferty M, Doyle MM, Nolan M, Preston RJS, Budde U, James P, Di Paola J, O'Donnell JS. Novel insights into the clinical phenotype and pathophysiology underlying low VWF levels. *Blood*. 2017;130:2344–53.

[24] Atiq F, Boender J, van Heerde WL, Tellez Garcia JM, Schoormans SC, Krouwel S, Cnossen MH, Laros-van Gorkom BAP, de Meris J, Fijnvandraat K, van der Bom JG, Meijer K, van Galen KPM, Eikenboom J, Leebeek FWG. Importance of genotyping in von Willebrand disease to elucidate pathogenic mechanisms and variability in phenotype. *Hemasphere*. 2022;6:e718. https://doi.org/10.1097/HS9.0000000000000718

[25] Swystun LL, Lillicrap D. Genetic regulation of plasma von Willebrand factor levels in health and disease. *J Thromb Haemost*. 2018;16:2375–90.

[26] de Boer S, Eikenboom J. Von Willebrand disease: from *in vivo* to in vitro disease models. *Hemasphere*. 2019;3:e297. https://doi.org/10.1097/HS9.0000000000000297

[27] Wang JW, Bouwens EA, Pintao MC, Voorberg J, Safdar H, Valentijn KM, de Boer HC, Mertens K, Reitsma PH, Eikenboom J. Analysis of the storage and secretion of von Willebrand factor in blood outgrowth endothelial cells derived from patients with von Willebrand disease. *Blood*. 2013;121:2762–72.

[28] Selvam SN, Casey LJ, Bowman ML, Hawke LG, Longmore AJ, Mewburn J, Ormiston ML, Archer SL, Maurice DH, James P. Abnormal angiogenesis in blood outgrowth endothelial cells derived from von Willebrand disease patients. *Blood Coagul Fibrinolysis*. 2017;28:521–33.

[29] Starke RD, Paschalaki KE, Dyer CE, Harrison–Lavoie KJ, Cutler JA, McKinnon TA, Millar CM, Cutler DF, Laffan MA, Randi AM. Cellular and molecular basis of von Willebrand disease: studies on blood outgrowth endothelial cells. *Blood*. 2013;121:2773–84.

[30] Laan SNJ, Lenderink BG, Eikenboom JCJ, Bierings R, SYMPHONY consortium. Endothelial colony-forming cells in the spotlight: insights into the pathophysiology of von Willebrand disease and rare bleeding disorders. *J Thromb Haemost*. 2024;22:3355–65.

[31] Bär I, Barraclough A, Bürgisser PE, van Kwawegen C, Fijnvandraat K, Eikenboom JCJ, Leebeek FWG, Voorberg J, Bierings R. The severe von Willebrand disease variant p.M771V leads to impaired anterograde trafficking of von Willebrand factor in patient-derived and base-edited endothelial colony-forming cells. *J Thromb Haemost*. 2025;23:466–79.

[32] de Wee EM, Sanders YV, Mauser-Bunschoten EP, van der Bom JG, Degenaar-Dujardin ME, Eikenboom J, de Goede–Bolder A, Laros-van Gorkom BA, Meijer K, Hamulyák K, Nijziel MR, Fijnvandraat K, Leebeek FW. WiN study group. Determinants of bleeding phenotype in adult patients with moderate or severe von Willebrand disease. *Thromb Haemost*. 2012;108:683–92.

[33] Rodeghiero F, Tosetto A, Abshire T, Arnold DM, Coller B, James P, Neunert C, Lillicrap D, ISTH/SSC joint VWF and Perinatal/Pediatric Hemostasis Subcommittees Working Group. ISTH/SSC bleeding

assessment tool: a standardized questionnaire and a proposal for a new bleeding score for inherited bleeding disorders. *J Thromb Haemost*. 2010;8:2063–5.

[34] de Boer S, Bowman M, Notley C, Mo A, Lima P, de Jong A, Dirven R, Weijers E, Lillicrap D, James P, Eikenboom J. Endothelial characteristics in healthy endothelial colony forming cells; generating a robust and valid *ex vivo* model for vascular disease. *J Thromb Haemost*. 2020;18:2721–31.

[35] Martin-Ramirez J, Hofman M, van den Biggelaar M, Hebbel RP, Voorberg J. Establishment of outgrowth endothelial cells from peripheral blood. *Nat Protoc*. 2012;7:1709–15.

[36] Laan SNJ, de Boer S, Dirven RJ, van Moort I, Kuipers TB, Mei H, Bierings R, Eikenboom J, SYMPHONY consortium. Transcriptional and functional profiling identifies inflammation and endothelial-to-mesenchymal transition as potential drivers for phenotypic heterogeneity within a cohort of endothelial colony forming cells. *J Thromb Haemost*. 2024;22:2027–38.

[37] Stirling DR, Swain–Bowden MJ, Lucas AM, Carpenter AE, Cimini BA, Goodman A. CellProfiler 4: improvements in speed, utility and usability. *BMC Bioinformatics*. 2021;22:433.

[38] Laan SNJ, Dirven RJ, Bürgisser PE, Eikenboom J, Bierings R. SYMPHONY consortium. Automated segmentation and quantitative analysis of organelle morphology, localization and content using CellProfiler. *PLOS One*. 2023;18:e0278009. https://doi.org/10.1371/journal.pone.0278009

[39] van Hooren KW, van Breevoort D, Fernandez-Borja M, Meijer AB, Eikenboom J, Bierings R, Voorberg J. Phosphatidylinositol-3,4,5-triphosphate-dependent Rac exchange factor 1 regulates epinephrine-induced exocytosis of Weibel–Palade bodies. *J Thromb Haemost*. 2014;12:273–81.

[40] de Jong A, Weijers E, Dirven R, de Boer S, Streur J, Eikenboom J. Variability of von Willebrand factor-related parameters in endothelial colony forming cells. *J Thromb Haemost*. 2019;17:1544–54.

[41] Groten SA, Smit ER, van den Biggelaar M, Hoogendijk AJ. The proteomic landscape of *in vitro* cultured endothelial cells across vascular beds. *Commun Biol*. 2024;7:989.

[42] Skowronek P, Thielert M, Voytik E, Tanzer MC, Hansen FM, Willems S, Karayel O, Brunner AD, Meier F, Mann M. Rapid and in-depth coverage of the (phospho-)proteome with deep libraries and optimal window design for dia-PASEF. *Mol Cell Proteomics*. 2022;21:100279. https://doi.org/10.1016/j.mcpro.2022.100279

[43] Maechler M, Rousseeuw P, Struyf A, Hubert M, Hornik K. cluster: cluster analysis basics and extensions. *R package*; 2023.https://CRAN.R-project.org/package=cluster.

[44] Ritchie ME, Phipson B, Wu D, Hu Y, Law CW, Shi W, Smyth GK. limma powers differential expression analyses for RNA-sequencing and microarray studies. *Nucleic Acids Res*. 2015;43:e47. https://doi.org/10.1093/nar/gkv007

[45] Phipson B, Lee S, Majewski IJ, Alexander WS, Smyth GK. Robust hyperparameter estimation protects against hypervariable genes and improves power to detect differential expression. *Ann Appl Stat*. 2016;10:946–63.

[46] Harrell FE Jr, Dupont C. Hmisc: harrell miscellaneous. R package version 5.1-4 20:2024. https://doi.org/10.32614/CRAN.package.Hmisc. [accessed July 20, 2025].

[47] Yu G, Wang LG, Han Y, He QY. clusterProfiler: an R package for comparing biological themes among gene clusters. *Omics*. 2012;16:284–7.

[48] James PD, Connell NT, Ameer B, Di Paola J, Eikenboom J, Giraud N, Haberichter S, Jacobs-Pratt V, Konkle B, McLintock C, McRae S, R Montgomery R, O'Donnell JS, Scappe N, Sidonio R, Flood VH, Husainat N, Kalot MA, Mustafa RA. ASH ISTH NHF WFH 2021 guidelines on the diagnosis of von Willebrand disease. *Blood Adv*. 2021;5:280–300.

[49] Sanders YV, Giezenaar MA, Laros-van Gorkom BA, Meijer K, van der Bom JG, Cnossen MH, Nijziel MR, Ypma PF, Fijnvandraat K, Eikenboom J, Mauser–Bunschoten EP, Leebeek FW, WiN study group. von Willebrand disease and aging: an evolving phenotype. *J Thromb Haemost*. 2014;12:1066–75.

[50] Rydz N, Grabell J, Lillicrap D, James PD. Changes in von Willebrand factor level and von Willebrand activity with age in type 1 von Willebrand disease. *Haemophilia*. 2015;21:636–41.

[51] Atiq F, Blok R, van Kwawegen CB, Doherty D, Lavin M, van der Bom JG, O'Connell NM, de Meris J, Ryan K, Schols SEM, Byrne M, Heubel–Moenen FCJI, van Galen KPM, Preston RJS, Cnossen MH, Fijnvandraat K, Baker RI, Meijer K, James P, Di Paola J, et al. Type 1 VWD classification revisited: novel insights from combined analysis of the LoVIC and WiN studies. *Blood*. 2024;143:1414–24.

[52] Starke RD, Ferraro F, Paschalaki KE, Dryden NH, McKinnon TA, Sutton RE, Payne EM, Haskard DO, Hughes AD, Cutler DF, Laffan MA, Randi AM. Endothelial von Willebrand factor regulates angiogenesis. *Blood*. 2011;117:1071–80.

[53] Groeneveld DJ, van Bekkum T, Dirven RJ, Wang JW, Voorberg J, Reitsma PH, Eikenboom J. Angiogenic characteristics of blood outgrowth endothelial cells from patients with von Willebrand disease. *J Thromb Haemost*. 2015;13:1854–66.

[54] Dai Y, Hu R, Liu A, Cho KS, Manuel AM, Li X, Dong X, Jia P, Zhao Z. WebCSEA: web-based cell-type-specific enrichment analysis of genes. *Nucleic Acids Res*. 2022;50:W782–90.

[55] Harvey NL, Srinivasan RS, Dillard ME, Johnson NC, Witte MH, Boyd K, Sleeman MW, Oliver G. Lymphatic vascular defects promoted by Prox1 haploinsufficiency cause adult-onset obesity. *Nat Genet*. 2005;37:1072–81.

[56] Wigle JT, Oliver G. Prox1 function is required for the development of the murine lymphatic system. *Cell*. 1999;98:769–78.

[57] Chen JM, Luo B, Ma R, Luo XX, Chen YS, Li Y. Lymphatic endothelial markers and tumor lymphangiogenesis assessment in human breast cancer. *Diagnostics (Basel)*. 2021;12:4.

[58] Zografou S, Basagiannis D, Papafotika A, Shirakawa R, Horiuchi H, Auerbach D, Fukuda M, Christoforidis S. A complete Rab screening reveals novel insights in Weibel-Palade body exocytosis. *J Cell Sci*. 2012;125:4780–90.

[59] Bierings R, Hellen N, Kiskin N, Knipe L, Fonseca AV, Patel B, Meli A, Rose M, Hannah MJ, Carter T. The interplay between the Rab27A effectors Slp4-a and MyRIP controls hormone-evoked Weibel–Palade body exocytosis. *Blood*. 2012;120:2757–67.

[60] Knop M, Aareskjold E, Bode G, Gerke V. Rab3D and annexin A2 play a role in regulated secretion of vWF, but not tPA, from endothelial cells. *EMBO J*. 2004;23:2982–92.

[61] van Breevoort D, van Agtmaal EL, Dragt BS, Gebbinck JK, Dienava–Verdoold I, Kragt A, Bierings R, Horrevoets AJ, Valentijn KM, Eikenboom JC, Fernandez–Borja M, Meijer AB, Voorberg J. Proteomic screen identifies IGFBP7 as a novel component of endothelial cell-specific Weibel–Palade bodies. *J Proteome Res*. 2012;11:2925–36.

[62] Truscott KN, Brandner K, Pfanner N. Mechanisms of protein import into mitochondria. *Curr Biol*. 2003;13:R326–37.

[63] Ma J, Hao Z, Zhang Y, Li L, Huang X, Wang Y, Chen L, Yang G, Li W. Physical contacts between mitochondria and WPBs participate in WPB maturation. *Arterioscler Thromb Vasc Biol*. 2024;44:108–23.

[64] Yamazaki Y, Eura Y, Kokame K. V-ATPase V0a1 promotes Weibel-Palade body biogenesis through the regulation of membrane fission. *Elife*. 2021;10:e71526. https://doi.org/10.7554/eLife.71526

[65] Terglane J, Menche D, Gerke V. Acidification of endothelial Weibel-Palade bodies is mediated by the vacuolar-type H+-ATPase. *PLOS One*. 2022;17:e0270299. https://doi.org/10.1371/journal.pone.0270299

[66] Medina RJ, O'Neill CL, O'Doherty TM, Chambers SE, Guduric–Fuchs J, Neisen J, Waugh DJ, Simpson DA, Stitt AW. *Ex vivo* expansion of human outgrowth endothelial cells leads to IL-8–mediated replicative senescence and impaired vasoreparative function. *Stem Cells*. 2013;31:1657–68.

[67] Smadja DM, Bièche I, Uzan G, Bompais H, Muller L, Boisson–Vidal C, Vidaud M, Aiach M, Gaussem P. PAR-1 activation on human late endothelial progenitor cells enhances angiogenesis in vitro with upregulation of the SDF-1/CXCR4 system. *Arterioscler Thromb Vasc Biol*. 2005;25:2321–7.

[68] Bompais H, Chagraoui J, Canron X, Crisan M, Liu XH, Anjo A, Tolla-Le Port C, Leboeuf M, Charbord P, Bikfalvi A, Uzan G. Human endothelial cells derived from circulating progenitors display specific functional properties compared with mature vessel wall endothelial cells. *Blood*. 2004;103:2577–84.

[69] Dejana E, Hirschi KK, Simons M. The molecular basis of endothelial cell plasticity. *Nat Commun*. 2017;8:14361. https://doi.org/10.1038/ncomms14361

[70] Potente M, Mäkinen T. Vascular heterogeneity and specialization in development and disease. *Nat Rev Mol Cell Biol*. 2017;18:477–94.

[71] Wigle JT, Harvey N, Detmar M, Lagutina I, Grosveld G, Gunn MD, Jackson DG, Oliver G. An essential role for Prox1 in the induction of the lymphatic endothelial cell phenotype. *EMBO J*. 2002;21:1505–13.

[72] Kilic N, Oliveira–Ferrer L, Neshat–Vahid S, Irmak S, Obst–Pernberg K, Wurmbach JH, Loges S, Kilic E, Weil J, Lauke H, Tilki D, Singer BB, Ergün S. Lymphatic reprogramming of microvascular endothelial cells by CEA-related cell adhesion molecule-1 via interaction with VEGFR-3 and Prox1. *Blood*. 2007;110:4223–33.

[73] Hickson N, Hampshire D, Winship P, Goudemand J, Schneppenheim R, Budde U, Castaman G, Rodeghiero F, Federici AB, James P, Peake I, Eikenboom J, Goodeve A, MCMDM-1VWD and ZPMCB-VWD study groups. von Willebrand factor variant p.Arg924Gln marks an allele associated with reduced von Willebrand factor and factor VIII levels. *J Thromb Haemost*. 2010;8:1986–93.

[74] Yin J, Ma Z, Su J, Wang JW, Zhao X, Ling J, Bai X, Ouyang W, Wang Z, Yu Z, Ruan C. Mutations in the D1 domain of von Willebrand factor impair their propeptide-dependent multimerization, intracellular trafficking and secretion. *J Hematol Oncol*. 2015;8:73.

[75] Penas N, Pérez–Rodríguez A, Torea JH, Lourés E, Noya MS, López–Fernández MF, Batlle J. von Willebrand disease R1374C: type 2A or 2M? A challenge to the revised classification. High frequency in the northwest of Spain (Galicia). *Am J Hematol*. 2005;80:188–96.

[76] Smith NL, Chen MH, Dehghan A, Strachan DP, Basu S, Soranzo N, Hayward C, Rudan I, Sabater–Lleal M, Bis JC, de Maat MP, Rumley A, Kong X, Yang Q, Williams FM, Vitart V, Campbell H, Mälarstig A, Wiggins KL, Van Duijn CM, et al. Novel associations of multiple genetic loci with plasma levels of factor VII, factor VIII, and von Willebrand factor: the CHARGE (Cohorts for Heart and Aging Research in Genome Epidemiology) Consortium. *Circulation*. 2010;121:1382–92.

[77] Sanders YV, van der Bom JG, Isaacs A, Cnossen MH, de Maat MP, Laros-van Gorkom BA, Fijnvandraat K, Meijer K, van Duijn CM, Mauser-Bunschoten EP, Eikenboom J, Leebeek FW, WiN Study Group. CLEC4M and STXBP5 gene variations contribute to von Willebrand factor level variation in von Willebrand disease. *J Thromb Haemost*. 2015;13:956–66.

[78] van Loon JE, Leebeek FW, Deckers JW, Dippel DW, Poldermans D, Strachan DP, Tang W, O'Donnell CJ, Smith NL, de Maat MP. Effect of genetic variations in syntaxin-binding protein-5 and syntaxin-2 on von Willebrand factor concentration and cardiovascular risk. *Circ Cardiovasc Genet*. 2010;3:507–12.

[79] Drakeford C, Aguila S, Roche F, Hokamp K, Fazavana J, Cervantes MP, Curtis AM, Hawerkamp HC, Dhami SPS, Charles–Messance H, Hackett EE, Chion A, Ward S, Ahmad A, Schoen I, Breen E, Keane J, Murphy R, Preston RJS, O'Sullivan JM, et al. von Willebrand factor links primary hemostasis to innate immunity. *Nat Commun*. 2022;13:6320. https://doi.org/10.1038/s41467-022-33796-7

[80] Cnossen MH, van Moort I, Reitsma SH, de Maat MPM, Schutgens REG, Urbanus RT, Lingsma HF, Mathot RAA, Gouw SC, Meijer K, Bredenoord AL, van der Graaf R, Fijnvandraat K, Meijer AB, van den Akker E, Bierings R, Eikenboom JCJ, van den Biggelaar M, de Haas M, Voorberg J, et al. SYMPHONY consortium: orchestrating personalized treatment for patients with bleeding disorders. *J Thromb Haemost*. 2022;20:2001–11.

SUPPLEMENTARY MATERIAL

The online version contains supplementary material available at https://doi.org/10.1016/j.jtha.2025.04.024